Design, Synthesis, Molecular Docking, and Anti-Inflammatory Evaluation of Novel Pyrazole-Schiff Base Hybrids as Potential COX-1/COX-2 Inhibitors

Shivam Jaiswal[1], Sujeet Kumar Gupta[2]*, Bhumika Yogi[3] and Nitin Mittal[4]
[1,4] Lords University, Alwar–Bhiwadi Highway, Chikani, Alwar – 301028, Rajasthan, India
[2,3] J.S Singh Institute of Pharmacy, Sitapur-261207, Uttar Pradesh, India
Corresponding author:
Dr Sujeet Kumar Gupta
Email id: sujeet20gupta2@gmail.com
Mob No. 9453409629

Abstract

Chronic inflammatory disorders remain a major global health challenge. Although cyclooxygenase (COX) inhibitors are widely used for anti-inflammatory therapy, the gastrointestinal toxicity of non-selective NSAIDs and the cardiovascular risks associated with selective COX-2 inhibitors necessitate the development of safer alternatives. In this study, a novel series of pyrazole-based Schiff base derivatives (S1–S10) was designed using a rational molecular hybridization approach by combining a pyrazole core, an isonicotinoyl moiety, an azomethine (Schiff base) linker, and a vanillin-derived 4-hydroxy-3-methoxyphenyl fragment to enhance anti-inflammatory potential. The target compounds were synthesized through hydrazone formation, Vilsmeier–Haack cyclization, and Schiff base condensation, and were characterized by IR, $_1$H NMR, and mass spectrometry. Molecular docking against COX-1 and COX-2 demonstrated favourable binding affinities for all synthesized compounds, with S9, S5, and S2 exhibiting the strongest interactions with the key Arg120 residue in the COX-2 active site. Anti-inflammatory activity was evaluated using the carrageenan-induced rat paw oedema model. The synthesized compounds produced significant, time-dependent inhibition of oedema, with S6 showing the highest inhibition (54.12% at 4 h) and S9 demonstrating the fastest onset of action, both displaying activity comparable to celecoxib. The strong agreement between molecular docking and in vivo findings suggests that COX-2 inhibition is the primary mechanism underlying the observed anti-inflammatory effects. These findings establish the pyrazole–isonicotinoyl–Schiff base hybrid scaffold as a structurally novel, well-tolerated, and pharmacologically promising.

Keywords: Pyrazole, Schiff base, Isonicotinoyl hydrazide, Molecular docking, Cyclooxygenase (COX-1/COX-2), Anti-inflammatory activity, Carrageenan induced paw oedema

How to cite this article: Jaiswal S, Gupta SK, Yogi B, Mittal N. Design, Synthesis, Molecular Docking, and Anti-Inflammatory Evaluation of Novel Pyrazole-Schiff Base Hybrids as Potential COX-1/COX-2 Inhibitors. Int J Drug Deliv Technol. 2026;16(71s): 176-186. DOI: 10.25258/ijddt.16.71s.21

1. Introduction

Inflammation is a basic biological response of the body to harmful stimuli such as pathogens, tissue injury, or irritants, and although acute inflammation is a protective and self-limiting process, its dysregulation or persistence leads to chronic inflammatory conditions that represent a major global health burden[1]. The most common and disabling of these are inflammatory musculoskeletal disorders such as rheumatoid arthritis and osteoarthritis. In 2021, osteoarthritis alone affected around 607 million people worldwide, making up about 7.7% of the world's population[2]. Rheumatoid arthritis, a chronic autoimmune inflammatory disease, affected an estimated 17.6 million individuals worldwide in 2020, with its age-standardised prevalence increasing by more than 14% since 1990. Both conditions disproportionately affect women and their disease burden continues to grow fastest in low and lower-middle income regions, reflecting a widening global treatment gap[3]. Beyond joint disease, chronic low-grade inflammation is now recognised as a central pathological driver in a wide range of disorders including cardiovascular disease, diabetes, neurodegeneration, and cancer, highlighting the broad clinical relevance of inflammatory pathways[4]. Therefore, the effective control of inflammation and the associated pain is still a mainstay of clinical therapeutics. These disorders are increasingly common and are chronic and progressive. In addition, existing anti-inflammatory therapies have limitations. Thus, there remains an unmet and growing medical need, providing strong impetus for the continued development of novel, safer and more effective anti-inflammatory agents.

Non-steroidal anti-inflammatory drugs (NSAIDs) are the most widely prescribed therapeutic agents for

the control of pain, fever and inflammation and have been in continuous clinical use since the 1960s. The main mechanism of their pharmacological action is to inhibit the cyclooxygenase (COX) enzyme system which catalyses the rate-limiting step in the biosynthesis of prostaglandins, thromboxanes and other eicosanoid mediators from arachidonic acid[5]. Two different isoforms of this enzyme have been characterised: COX-1, which is constitutively expressed in most tissues and subserves homeostatic "housekeeping" functions such as maintenance of gastric mucosal integrity, regulation of renal blood flow, and platelet aggregation, and COX-2, an inducible isoform whose expression is significantly upregulated at sites of tissue injury and is largely responsible for the generation of pro-inflammatory prostaglandins that drive the classical signs of inflammation. (aspirin, ibuprofen, diclofenac and naproxen) are non-selective conventional NSAIDs and inhibit both COX-1 and COX-2[6]; This dual inhibition is effective in suppressing inflammation and pain, but the concomitant blockade of protective COX-1-derived prostaglandins in the gastric mucosa compromises mucosal defence mechanisms, predisposing patients to a well-documented spectrum of gastrointestinal complications from dyspepsia and mucosal erosion to frank peptic ulceration, haemorrhage and perforation, particularly with long-term or high dose use[7]. Epidemiological data from the pre-coxib era consistently showed NSAID-induced gastropathy to be a major reason for drug-related hospitalisation, which led to a sustained search for agents that could retain anti-inflammatory efficacy but spare the gastrointestinal tract[8].

This search led to the rational design of selective COX-2 inhibitors, colloquially known as "coxibs," that were designed to preferentially occupy the larger and more accommodating active site of COX-2, sparing COX-1 and its cytoprotective functions. The first agent of this class to reach the market was celecoxib, introduced in 1998, and this was followed shortly thereafter by rofecoxib in 1999; these drugs rapidly achieved widespread clinical adoption due to their demonstrably reduced incidence of gastrointestinal adverse effects relative to conventional NSAIDs[9]. For a time, coxibs seemed to be a real therapeutic breakthrough, providing effective anti-inflammatory and analgesic action without the ulcerogenic burden of their non-selective predecessors. But this apparent success lasted but a short time. Initial trials, such as VIGOUR, provided convincing evidence of the gastrointestinal safety benefit of rofecoxib but at the same time raised concerns about cardiovascular toxicity with the risk of myocardial infarction being considerably higher relative to naproxen [10]. These findings were confirmed and extended in later, larger trials. The Vioxx Gastrointestinal Outcomes Research (VIGOUR) study and the Adenomatous Polyp Prevention on Vioxx (APPROVe) study both showed a significantly increased risk of serious cardiovascular events with rofecoxib, a finding that ultimately resulted in the manufacturer withdrawing the drug from the worldwide market in September 2004. The magnitude of harm attributed to this single agent was staggering: rofecoxib has been retrospectively estimated to have caused more than 88,000 cases of myocardial infarction and more than 38,000 deaths in the United States alone during its period of clinical use[11-12]. The mechanistic basis for this cardiovascular liability has since been attributed to disruption of the physiological balance between thromboxane A2, a pro-thrombotic and vasoconstrictive mediator generated via COX-1 in platelets, and prostacyclin (PGI2), an antithrombotic and vasodilatory mediator generated via COX-2 in vascular endothelium; selective COX-2 inhibition suppresses prostacyclin synthesis while leaving thromboxane production intact, thereby tilting haemostasis toward a prothrombotic state[13]. Rofecoxib was not a one-off; valdecoxib was withdrawn from the market for similar cardiovascular concerns and celecoxib, although it has survived regulatory approval, has been subject to significant scrutiny, litigation and boxed-warning labelling for its own cardiovascular safety profile[14-15]. This sequence of events revealed a fundamental and as yet unresolved therapeutic dilemma at the heart of COX-directed pharmacology: the very structural and pharmacodynamic modifications that confer gastrointestinal safety through COX-2 selectivity seem to simultaneously predispose patients to cardiovascular harm[16]. As a result, clinicians today are often challenged to balance gastrointestinal risk with cardiovascular risk when choosing an anti-inflammatory agent, particularly in older patients or those with pre-existing comorbidities, where both risks are magnified. This unresolved trade-off, compounded by the reality that no currently marketed COX inhibitor is universally safe across all patient populations, constitutes the central pharmacological "gap" that continues to drive medicinal chemistry efforts toward the design of structurally novel anti-inflammatory agents capable of achieving a more favourable balance between efficacy and safety — an objective that directly motivates the present study.

In the quest for safer and more effective anti-inflammatory chemotherapeutics, the pyrazole nucleus, a five-membered aromatic heterocycle containing two adjacent nitrogen atoms, has emerged as one of the most extensively investigated and pharmacologically privileged scaffolds in medicinal chemistry. Pyrazole derivatives have been reported to possess an exceptionally broad spectrum of biological activities, such as anti-inflammatory[17-19], antipyretic, analgesic[20], antimicrobial, anticancer, antitubercular, antiviral, antihypertensive, antioxidant, antidepressant and

antidiabetic properties, a breadth of pharmacological action rarely matched by other heterocyclic systems[21]. This remarkable versatility is generally attributed to the ring's favourable physicochemical characteristics — its aromatic, planar geometry, moderate lipophilicity, metabolic stability, and the presence of two nitrogen atoms capable of participating in hydrogen bonding and other key interactions with diverse biological targets — which together allow substituted pyrazoles to be readily accommodated within a wide range of enzyme active sites [22].

The pyrazole ring is of specific importance in the field of anti-inflammatory drug design, being most notably the structural core of celecoxib itself – the very drug that pioneered the selective COX-2 inhibitor class discussed above. The planar, lipophilic shape of the 1,5-diarylpyrazole scaffold in celecoxib allows it to fit efficiently into the larger, hydrophobic side-pocket that is unique to the COX-2 active site, a structural trait that accounts significantly for its isoform selectivity, as compared to COX-1 [23]. Besides celecoxib, a number of other pyrazole-containing COX-2-directed agents of clinical or investigational importance have been reported. These include the widely used pyrazole-containing COX-2 selective research probe, SC-558 . More generally, pyrazole derivatives have continued to show significant therapeutic potential in treating inflammation via selective COX-2 inhibition, indicating ongoing interest in medicinal chemistry in this scaffold as a platform for the rational design of next-generation coxibs [24]. A number of novel pyrazole-based derivatives with sulfonamide, carboxamide and other pharmacophoric appendages have been reported in recent years, with COX-2 selectivity indices greater than that of celecoxib itself, good in vivo anti-inflammatory activity and reduced ulcerogenic liability in animal models, showing that the pyrazole core is still a productive template for structural optimisation rather than a historical curiosity [25-26].

Pyrazole rings with an azomethine (Schiff base) functionality have received increasing attention as a distinct and pharmacologically fertile sub-class within this family, which is especially relevant to the current study. Pyrazole–Schiff base hybrids have been reported to show significant anti-inflammatory activity via COX-2 inhibition, with at least one such derivative displaying nanomolar-range COX-2 inhibitory potency along with a favourable selectivity index over COX-1 and a substantial reduction in paw oedema upon in vivo evaluation. Other pyrazole–Schiff base derivatives have been also reported for antibacterial and anticancer activity, evidencing the multi-target pharmacological potential of this hybrid chemotype [27]. Together, this extensive body of literature evidence validates the pyrazole ring as much more than a synthetically convenient bioisostere: it is a pharmacologically validated, target-engaging core with a proven ability to productively interact with the COX enzyme system, while at the same time providing a versatile synthetic handle – most notably via pendant carbonyl or hydrazide functionalities – for further structural elaboration into Schiff base and other hybrid pharmacophores. The rationale for the selection of the pyrazole ring as the central scaffold of the compounds designed, synthesised and evaluated in the present study is precisely the dual advantage of established COX-directed bioactivity and synthetic versatility.

The Schiff base, synthesised by condensation of a primary amine with an aldehyde, giving an azomethine (-C=N-) linkage, is a privileged pharmacophore in medicinal chemistry. Schiff bases are known as flexible frameworks for the development of bioactive leads, showing anti-inflammatory, analgesic, antimicrobial, anticonvulsant, antitubercular, anticancer, antioxidant and antidepressant activities [14]. The versatility of this is mainly based on the lone pair of the azomethine nitrogen providing the hydrogen-bond acceptor properties and good geometrical interactions with different biological targets [15].

Azomethine functionality has been directly associated with anti-inflammatory activity, specifically for this investigation. The mono-imine Schiff bases showed very strong anti-inflammatory activity and the electronics of the substituent was shown to modulate the potency [28]. More importantly, azomethine-linked pyrazole-sulfonamide hybrids have shown nanomolar COX-2 inhibition with good selectivity for COX-1, as well as significant reduction of carrageenan-induced paw oedema in vivo. This precedent confirms that the Schiff base linkage, when positioned on a pyrazole core, is not just a synthetic convenience but an independently validated contributor to COX-directed anti-inflammatory activity, justifying its selection as the key connecting pharmacophore in the present molecular design.

Molecular hybridisation was employed to design the title compounds, a rational strategy that combines pharmacologically validated fragments into a single molecule to obtain complementary or synergistic activity [29]. Four elements were incorporated: a pyrazole core, a N1-isonicotinoyl (pyridine-4-carbonyl) group, a C4-azomethine bridge and a terminal vanillin-derived 4-hydroxy-3-methoxyphenyl ring.

The pyrazole core was selected for its known affinity for the binding site of COX, as in the case of celecoxib [30]. The isonicotinoyl group was included based on the precedent of isoniazid-hybrid docking: the pyridine nitrogen and adjacent carbonyl oxygen have been shown to form coordinated hydrogen bonds with key active-site residues, improving binding affinity, while the pyridine ring itself occupies a hydrophobic binding pocket consistently

[19,20]. This recurring hydrogen-bonding/hydrophobic-anchoring behaviour justified keeping isonicotinoyl at N1 instead of an unfunctionalised acyl group.

Specifically, the vanillin-type terminus was retained for its independent anti-inflammatory and antioxidant contribution. Vanillin derivatives have exhibited considerable analgesic and anti-inflammatory activity in carrageenan-induced paw oedema models, mechanistically linked to TRPA1/TRPV1 modulation [31], whereas the free phenolic hydroxyl group is able to scavenge reactive oxygen species, attenuating downstream inflammatory signalling [32-33].

Collectively, this hybrid architecture was engineered so that each fragment contributes a distinct, literature-supported function — COX engagement (pyrazole), target anchoring via hydrogen bonding (isonicotinoyl), synthetic/pharmacophoric versatility (azomethine), and complementary antioxidant activity (vanillin moiety) — forming the rational basis for compounds 4a–j, further probed here through molecular docking against COX-1 and COX-2.

Material and Methods

The melting points were determined in open capillary tubes with a digital melting point apparatus and are reported uncorrected, in °C. The progress of the reaction was followed by TLC on pre-coated silica gel plates using petroleum ether:ethyl acetate (9:1, v/v) as mobile phase, spots visualised under UV light at 254 nm. All the synthesised compounds were characterised by physical and spectral analysis. ^{1}H NMR spectra were recorded on a Bruker Avance 300 MHz spectrometer. DMSO-d6 was used as solvent and chemical shifts are reported in δ (ppm). IR spectra were recorded as KBr pellets and absorptions are given in cm^{-1}. All chemicals used were of synthetic grade and were obtained from Merck, Sigma Aldrich and other standard commercial suppliers.

Experimental Section

Preparation of Isonicotino Hydrazones (3)

A solution of 4'-hydroxy-3'-methoxyacetophenone (3.5 mmol) in glacial acetic acid (20 mL) was prepared with continuous stirring. Then, isonicotinohydrazide (3.5 mmol) was added dropwise to the mixture at room temperature. Stirring was continued for a further 5 min during which time a pale yellow to off-white solid separated out of solution. The precipitate was collected by filtration, washed extensively with distilled water to eliminate residual impurities, and dried under vacuum to afford the target hydrazone.

Pale yellow crystalline powder, Yield: 76%, M.P. 221°C, R_f: 0.37 ($CHCl_3$: MeOH (9:1)), CF/MWt: $C_{15}H_{15}N_3O_3$/285; IR (Kbr, cm^{-1}): 3398.09 (C-OH), 3201.83 (N-H) 3054.88 (Ar C-H), 2964.72 (Ali C-H), 1669.09 (C=O), 1590.72 (C=N), 1512.03 (Ar C-C), 1225.58 (C-N), 1112.49 (N-N), 1071.84 (C-O-C); ^{1}H-NMR (300 MHz, δ in ppm): 2.32 (s, 3H, CH_3), 4.411 (s, 3H, OCH_3), 7.299-8.344 (m, 7H, Ar-H), 9.55 (s, 1H, O-H), 11.58 (s, 1H, NH); Mass (*e/z*): 286.45 [M+1]

Preparation of 3-(4-hydroxy-3-methoxyphenyl)-1-isonicotinoyl-1H-pyrazole-4-carbaldehyde (4)

A solution of (E)-N′-(1-(4-hydroxy-3-methoxyphenyl)ethylidene)isonicotinohydrazide (3) (1.2 mmol) in dimethylformamide (DMF, 15 mL) was cooled to 0 °C in an ice bath. Phosphorus oxychloride (POCl3, 7.2 mmol, 6 equiv) was added dropwise over 10 min, keeping the temperature at 0 °C during addition. The reaction mixture was then heated to reflux (85–90 °C) and maintained under reflux for 1 h. On completion, the mixture was poured cautiously onto crushed ice and neutralized with 10% aqueous NaOH solution. The product was extracted into dichloromethane (3 × 30 mL), and the combined organic extracts were washed repeatedly with distilled water (5–6 washes), dried over anhydrous Na2SO4, and concentrated under reduced pressure. The crude residue was purified by silica gel column chromatography (petroleum ether:ethyl acetate, 9:1 v/v) to afford the title compound (3) 1-isonicotinoyl-3-(4-hydroxy-3-methoxyphenyl)-1H-pyrazole-4-carbaldehyde.

Yellow crystalline, Yield: 66%, M.P. 197°C, R_f: 0.43 (PE:EA, 9:1); CF/MWt: $C_{17}H_{13}N_3O_4$/ 332; IR (Kbr, cm^{-1}): 3395.28 (C-OH), 2731.60 (Ald C-H), 1706.31 (Ald C=O), 1625.62 (amide C=O), 1382.51 (C-N), 1317.31 (Pyridine C-N), 1262.39 (C-O), 1073.35 (N-N); ^{1}H-NMR (300 MHz, δ in ppm): 3.87 (s, 3H, OCH_3), 7.12-8.34 (m, 8H, Ar-H), 9.74 (s, 1H, HC=N), 10.41 (s, 1H, OH); Mass (*e/z*): 324.57 (M+1)

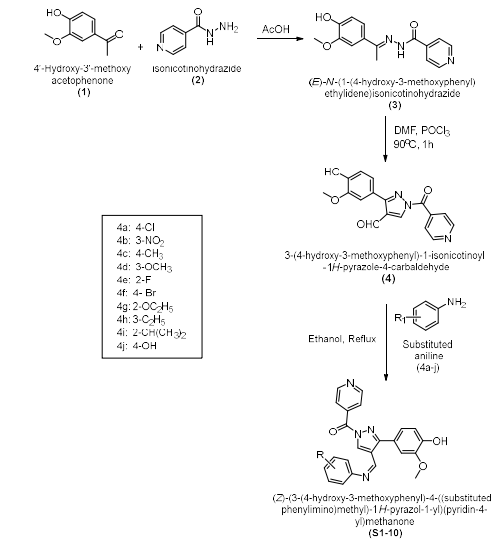

Fig 1. Scheme for designed derivative (S1-S10)

General procedure for (*Z*)-(3-(4-hydroxy-3-methoxyphenyl)-4-((substitutedphenylimino) methyl)-1*H*-pyrazol-1-yl)(pyridin-4-yl)methanonev (S1-10)

A mixture of 3-(4-hydroxy-3-methoxyphenyl)-1-isonicotinoyl-1H-pyrazole-4-carbaldehyde (3) (1 mmol) and the corresponding substituted aniline (1 mmol) was dissolved in absolute ethanol (20 mL). Glacial acetic acid (2-3 drops) was introduced as a catalyst, and the mixture was heated under reflux for 3-4 h. Reaction progress was monitored by thin-layer chromatography (TLC) using an appropriate solvent system, and heating was continued until the starting aldehyde was fully consumed. The mixture was then allowed to cool to room temperature, resulting in the formation of a solid precipitate. The Schiff base product was isolated by vacuum filtration, washed with cold ethanol to remove unreacted starting materials, and dried under reduced pressure. Recrystallization from absolute ethanol afforded the pure pyrazole-based Schiff base derivatives (4a-j).

(E)-(4-(((4-chlorophenyl)imino)methyl)-3-(4-hydroxy-3-methoxyphenyl)-1H-pyrazol-1-yl)(pyridin-4-yl)methanone (S1)

Pale yellow crystalline powder, Yield: 80%, M.P. 198-200°C, R_f: 0.57 (PE:EA 9:1), CF/MWt: $C_{23}H_{17}ClN_4O_3$/432.86; IR (Kbr, cm^{-1}): 3402.24 (C-OH), 1689.80 (C=O), 1600.60 (C=N), 1298.11 (Pyridine C-N), 1258.69 (N-C), 1138.96 (C-OCH_3), 1072.31 (N-N), 744.91 (C-Cl); ^{1}H-NMR (300 MHz, δ in ppm): 4.21 (s, 3H, OCH_3), 7.02-8.83 (m, 12H, Ar-H), 8.87 (s, 1H, HC=N), 10.24 (s, 1H, OH); Mass (*e/z*): 432.8 (M+), 434.1 (M+1)

(E)-(3-(4-hydroxy-3-methoxyphenyl)-4-(((3-nitrophenyl)imino)methyl)-1H-pyrazol-1-yl)(pyridin-4-yl)methanone (S2)

Yellow crystalline powder, Yield: 70%, M.P. 211-213°C, R_f: 0.42 (PE:EA 9:1), CF/MWt: $C_{23}H_{17}N_5O_5$/443.4; IR (Kbr, cm-1): 3352.07 (C-OH), 3069.99 (Ar C-H), 1675.84 (C=O), 1596.79 (C=N), 1391.94 (NO2), 1329 (Pyridine C-N), 1248.38 (N-C), 1084.50 (C-OCH_3), 1006.29 (N-N); ^{1}H-NMR (300 MHz, δ in ppm): 3.98 (s, 3H, OCH3), 6.78-8.12 (m, 12H, Ar-H), 8.91 (s, 1H, HC=N), 10.11 (s, 1H, OH); Mass (e/z): 444.51 (M+1)

(E)-(3-(4-hydroxy-3-methoxyphenyl)-4-((p-tolylimino)methyl)-1H-pyrazol-1-yl)(pyridin-4-yl)methanone (S3)

Pale yellow crystalline powder, Yield: 83%, M.P. 183-185°C, Rf: 0.62 (PE:EA 9:1), CF/MWt: $C_{24}H_{20}N_4O_3$/412.44; IR (Kbr, cm^{-1}): 3399.70 (C-OH), 3083.89 (Ar C-H), 2928.52 (Ali C-H), 1713.26 (C=O), 1619.48 (C=N), 1386.21 (Pyridine C-N), 1160.95 (OCH_3), 1098.42 (N-N); ^{1}H-NMR (300 MHz, δ in ppm): 2.37 (s, 3H, -CH3), 4.24 (s, 3H, OCH_3), 6.68-8.14 (m, 12H, Ar-H), 9.23 (s, 1H, HC=N), 10.38 (s, 1H, O-H). Mass (*e/z*): 413.59 (M+1)

(E)-(3-(4-hydroxy-3-methoxyphenyl)-4-(((3-methoxyphenyl)imino)methyl)-1H-pyrazol-1-yl)(pyridin-4-yl)methanone (S4)

Yellow crystalline powder, Yield: 76%, M.P. 196-198°C, Rf: 0.52 (PE:EA 9:1), CF/MWt: $C_{24}H_{20}N_4O_4$/428.45; IR (Kbr, cm^{-1}): 3402.36 (C-OH), 2915.40 (Ali C-H), 1681.23 (C=O), 1635.53 (C=N), 1391.18 (N-C), 1170.11 (OCH_3), 1006.62 (N-N); ^{1}H-NMR (300 MHz, δ in ppm): 3.87 (s, 3H, OCH_3), 4.09 (s, 3H, OCH_3), 6.61-8.47 (m, 12H, Ar-H), 8.95 (s, 1H, HC=N), 10.42 (s, 1H, OH); Mass (*e/z*): 428.1 (M+), 429.81 (M+1)

(E)-(4-(((2-fluorophenyl)imino)methyl)-3-(4-hydroxy-3-methoxyphenyl)-1H-pyrazol-1-yl)(pyridin-4-yl)methanone (S5)

Light Brown crystalline powder, Yield: 75%, M.P. 190°C, R_f: 0.57 (PE:EA 9:1), CF/MWt: $C_{23}H_{17}FN_4O_3$/416.4; IR (Kbr, cm^{-1}): 3362.83 (C-OH), 2929.83 (Ali C-H), 1699.85 (C=O), 1644.40 (C=N), 1313.17 (N-C), 1254.10 (OCH_3), 1142.73 (C-F), 1067.99 (N-N); ^{1}H-NMR (300 MHz, δ in ppm): 4.35 (s, 3H, CH_3), 6.76-8.36 (m, 12H, Ar-H), 8.48 (s, 1H, HC=N), 10.22 (s, 1H, OH); Mass (*e/z*): 417.8 (M+1)

(E)-(4-(((4-bromophenyl)imino)methyl)-3-(4-hydroxy-3-methoxyphenyl)-1H-pyrazol-1-yl)(pyridin-4-yl)methanone (S6)

Yellow crystalline powder, Yield: 80%, M.P. 205-207°C, Rf: 0.57 (PE:EA 9:1), CF/MWt: $C_{23}H_{17}BrN_4O_3$/477.31; IR (Kbr, cm^{-1}): 3359.06 (C-OH), 1684.32 (C=O), 1615.88 (C=N), 1524.03 (Ar C-C), 1347.02 (N-C), 1220.15 (OCH_3), 586.37 (C-Br); ^{1}H-NMR (300 MHz, δ in ppm): 4.17 (s, 3H, OCH_3), 6.79-8.12 (m, 12H, Ar-H), 8.44 (s, 1H, HC=N), 10.54 (s, 1H, OH); Mass (*e/z*): 478.9 (M+1)

(E)-(4-(((2-ethoxyphenyl)imino)methyl)-3-(4-hydroxy-3-methoxyphenyl)-1H-pyrazol-1-yl)(pyridin-4-yl)methanone (S7)

Pale Yellow crystalline powder, Yield: 75%, M.P. 175-177°C, Rf: 0.52 (PE:EA 9:1), CF/MWt: $C_{25}H_{22}N_4O_4$/442.47; IR (Kbr, cm^{-1}): 3402.94 (C-OH), 2921.01 (Ali C-H), 1701.73 (C=O), 1600.13 (C=N), 1325.01 (N-C), 1261.34 (OCH_3), 1139.15 (C-O), 1065.23 (N-N); ^{1}H-NMR (300 MHz, δ in ppm): 1.37 (s, 3H, Ali H), 3.53 (s, 3H, OCH_3), 4.28 (s, 2H, -CH_2-), 6.79-8.34 (m, 12H, Ar-H), 9.01 (s, 1H, HC=N), 10.87 (s, 1H, OH); Mass (*e/z*): 443.8 (M+1)

(E)-(4-(((3-ethylphenyl)imino)methyl)-3-(4-hydroxy-3-methoxyphenyl)-1H-pyrazol-1-yl)(pyridin-4-yl)methanone (S8)

Pale yellow crystalline powder, Yield: 83%, M.P. 180°C, Rf: 0.62 (PE:EA 9:1), CF/MWt: $C_{25}H_{22}N_4O_3$/426.47; IR (Kbr, cm^{-1}): 3439.14 (C-OH), 2922.39 (Ali C-H), 1674.79 (C=O), 1617.00 (C=N), 1585.44 (Ar C-H), 1311.87 (N-C), 1242.57 (OCH_3), 1068.52 (N-N); ^{1}H-NMR (300 MHz, δ in ppm): 1.21 (s, 3H, Ali H), 2.73 (s, 2H, -CH_2-), 3.84 (s, 3H, CH_3), 6.83-8.24 (m, 12H, Ar-H), 8.89 (s, 1H, HC=N), 9.88 (s, 1H, OH); Mass (*e/z*): 427.8 (M+1)

(E)-(3-(4-hydroxy-3-methoxyphenyl)-4-(((3-isopropylphenyl)imino)methyl)-1H-pyrazol-1-yl)(pyridin-4-yl)methanone (S9)

Pale yellow crystalline powder, Yield: 77%, M.P. 170°C, Rf: 0.65 (PE:EA 9:1), CF/MWt: $C_{26}H_{24}N_4O_3$/440.50; IR (Kbr, cm^{-1}): 3332.61 (C-OH), 3068.80 (Ar C-H), 2914.85 (Ali C-H), 1675.83 (C=O), 1644.06 (C=N), 1545.53 (Ar C-C), 1327.77 (N-C), 1239.88 (OCH_3), 1065.19 (N-N); ^{1}H-NMR (300 MHz, δ in ppm): 1.25 (s, 3H, Ali H), 1.42 (s, 3H, Ali H), 2.95 (s, 1H, -CH-), 4.12 (s, 3H, OCH_3), 6.65-8.40 (m, 12H, Ar-H), 8.77 (s, 1H, HC=N), 10.33 (s, 1H, OH); Mass (*e/z*): 441.7 (M+1)

(E)-(3-(4-hydroxy-3-methoxyphenyl)-4-(((4-hydroxyphenyl)imino)methyl)-1H-pyrazol-1-yl)(pyridin-4-yl)methanone (S10)

Deep yellow crystalline powder, Yield: 66%, M.P. 230°C, Rf: 0.34 (PE:EA 9:1), CF/MWt: $C_{23}H_{18}N_4O_4$/414.42; IR (Kbr, cm^{-1}): 3432.08 (C-OH), 3012.27 (Ar C-C), 2929.83 (Ali C-H), 1689.23 (C=O), 1609.85 (C=N), 1254.10 (N-C), 1142.73 (OCH_3), 1067.99 (N-N); ^{1}H-NMR (300 MHz, δ in ppm): 4.27 (s, 3H, OCH_3), 6.83-8.76 (m, 12H, Ar-H), 8.94 (s, 1H, HC=N), 9.41 (s, 1H, OH), 10.2 (s, 1H, OH); Mass (*e/z*): 414.5 (M+), 415.8 (M+1)

Docking analysis

To rationalise the anti-inflammatory potential of synthesised pyrazole-Schiff base derivatives (S11–S20), in silico molecular docking was performed against cyclooxygenase-1 (COX-1, PDB: 6Y3C) and cyclooxygenase-2 (COX-2, PDB: 5KIR) retrieved from RCSB Protein Data Bank. Polar hydrogens and Kollman charges were added after removal of co-crystallized water and heteroatoms from protein structures. Ligand structures were sketched and energy minimised before docking. Docking was carried out using AutoDock Vina, with the grid box centered on the catalytic active site of each enzyme, and the protocol was validated by re-docking the co-crystallized ligand to reproduce its native binding pose. Reference standard for COX-1 was Flurbiprofen and for COX-2 was Rofecoxib. Interaction analysis was performed by Discovery Studio Visualiser after docking. All ten derivatives showed binding affinities of −7.3 to −8.2 kcal/mol against COX-1 and −7.9 to −9.0 kcal/mol against COX-2, with every compound outperforming both reference drugs (flurbiprofen, −6.4; rofecoxib, −6.8 kcal/mol).

Table 1. Molecular docking results of novel synthesized compounds against COX-1, PDB: 6Y3C and COX-2, PDB: 5KIR.

Compound	COX-I Binding Affinity (kcal/mol)	Key Amino Acid Residues	H-Bonds	COX-II Binding Affinity (kcal/mol)	Key Amino Acid Residues	H-Bonds
S1	-7.9	Arg 83, Val 119 & 116, Leu 115 & 123, Pro 86, Tyr 64		-8.3	Phe 470	Val 89, Leu 93, Ile 92, Trp 100, Pro 86, Lys 83 & 79	Glu 524
S2	-8.2	Arg 79, Pro 86, Leu 123, Val 116 & 119, Leu 115		-8.1	Phe 470, Arg 83	Try 115, Arg 120, Val 116, 89, Leu 93, Ile 92, Lys 83 & 79	Glu 524
S3	-7.9	Arg 83, Val 119 & 116, Leu 115 & 123, Pro 86, Arg 79, Tyr 64		-8.5	Glu 524	Val 89, Trp 100, Ile 92, Leu 93, Lys 79 & 83, Pro 86	Arg 120
S4	-7.3	Glu 524, Arg 83, Val		-8.0	Arg 79	Val 89, Leu 93, Lys 79	-

		119, Pro 86			& 83, Met 471	
S5	-8.1	Val 116 & 119 Leu 115 & 123, Arg 83, Glu 524	Phe 470	-8.9	Val 89, Leu 93, Lys 79 &83, Tyr 115	Arg 120
S6	-8.1	Leu 115, Arg 83, Tyr 64, Leu 123, Val 116 & 119	Gly 471	-8.2	Ser 579	His 356 & 351, Ser 581, Phe 580
S7	-7.5	Val 119, Arg 79	Arg 83, Ans 122	-7.9	Val 89 & 116, Tyr 115, Leu 93, Arg 120, Lys 83	Glu 524
S8	-7.7	Arg 83, Leu 123 & 115, Pro 86, Val 119	Phe 470	-8.2	Val 89, Lys 79 & 83, Met 471, Leu 93	-
S9	-8.2	Glu 542,	Phe 470,	-9.0	Val 89, Pro	Arg 120
		Arg 83, Leu 123 & 115, Pro 86, Val 119	Gly 471		86, Ile 92, Trp 100, Ile 112, Leu 93, Lys 79 & 83	
S10	-8.1	Leu 123 & 115, Pro 86, Val 119 & 116, Arg 79	Ans 80, Tyr 64, Phe 470	-8.1	Val 89, Pro 86, Leu 93, Lys 79 & 83	Arg 120
Std.	-6.4 (Flurbiprofen)	Trp 100, Leu 112, Leu 93		-6.8 (Rofecoxib)	-	Asn 350, Phe 580, Ser 581

Compounds S2 and S9 were the strongest binders (−8.2 kcal/mol) against COX-1, followed by S5, S6, and S10 (−8.1 kcal/mol), and S14 was the weakest (−7.3 kcal/mol). Consistent hydrophobic contacts were observed with Val116/Val119, Leu115/Leu123, Arg83, and Pro86 across the series, while hydrogen bonding was most frequently mediated through Phe470 (S1, S2, S6, S8–S10) and Arg79 (S3, S4, S7). S9 presented the highest binding energy against COX-2 (−9.0 kcal/mol), followed by S5 (−8.9) and S3 (−8.5), sharing a hydrophobic footprint of Val89, Leu93, Ile92 and Lys79/Lys83. A hydrogen bond with Arg120 — a residue central to polar-group recognition at the COX-2 substrate channel, and the same interaction exploited by celecoxib and rofecoxib — was observed for most of the top-binding compounds (S2, S5, S9, S10), suggesting this interaction as a key driver of enhanced COX-2 affinity. S6 was an exception, which engaged His351/His356 and Ser579/Ser581 instead, suggesting a different binding mode.

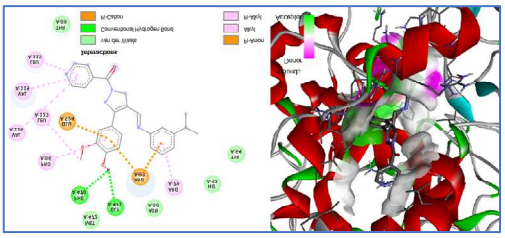

Fig 2. The 3D and 2D binding interactions of compound S19 with Cyclooxygenase-1 (COX-1, PDB: 6Y3C).

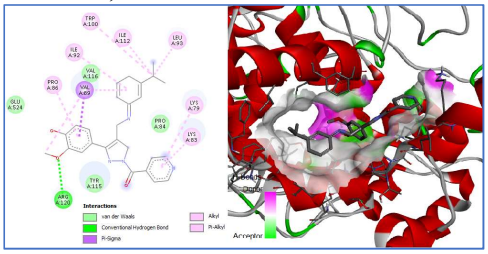

Fig 3. The 3D and 2D binding interactions of compound S19 with Cyclooxygenase-2 (COX-2, PDB: 5KIR)

Pharmacological activity of Pyrazole-Schiff Base Hybrids

Acute Toxicity Study

The acute oral toxicity of synthesised derivatives (S1–S10) was studied according to OECD Guideline 425 (Up-and-Down Procedure) after institutional ethical clearance and following CPCSEA guidelines. Healthy adult female Wistar albino rats (non pregnant, nulliparous) weighing 100-150 g were used. The rats were fasted overnight with free access to water and weighed before dosing . The test compound was administered orally as a suspension in 0.5% w/v CMC at a starting dose level of 2000 mg/kg body weight. Animals were observed continuously for the first 4 hours post dosing and periodically during the next 24 hours and then once daily for 14 days. Observations included changes in skin and fur, eyes and mucous membranes, respiration, autonomic and central nervous system effects, behaviour, body weight and mortality. Dosing was then conducted in accordance with the OECD 425 up-and-down sequence. None of the derivatives (S1-S10) at the tested dose level of 2000 mg/kg produced mortality or any sign of toxicity during the 14-day observation period. The animals of the treated groups remained normal in their behaviour and there was no significant change in the body weight or the gross parameters as compared to the control . According to OECD 425 all compounds are classified in toxicity Category 5 (LD50 > 2000 mg/kg). From this good safety margin, 1/10 and 1/5 of the maximum non lethal dose (50 and 100 mg/kg respectively) were selected as the therapeutic dose range for the further anti-inflammatory evaluation.

Carrageenan-Induced Paw Edema Assay

The in vivo anti-inflammatory potential of the synthesized derivatives (S1–S10) was evaluated by carrageenan-induced hind paw edema in rats, following the method of Winter et al. with slight modifications. Healthy adult Wistar albino rats of either sex, weighing 100–150 g, were procured from the institutional animal house and acclimatized for one week under standard housing conditions (25 ± 2 °C, 55 ± 10% relative humidity, 12 h light/dark cycle) with free access to standard pellet diet and water ad libitum. All experimental protocols were approved by the Institutional Animal Ethics Committee (IAEC) and conducted in accordance with CPCSEA guidelines, Government of India. Animals were randomly divided into groups comprising a carrageenan (disease) control receiving vehicle alone, a standard group treated orally with celecoxib (10 mg/kg), and treatment groups receiving the test compounds S1–S10 orally at their respective doses (2.5, 5.0, or 10.0 mg/kg body weight), each suspended in 0.5% w/v carboxymethyl cellulose (CMC) and administered one hour prior to the phlogistic challenge. Acute paw inflammation was induced by sub-plantar injection of 0.1 mL of 1% w/v carrageenan suspension in normal saline into the right hind paw of each rat. Paw volume was measured at 0 h (pre-injection, baseline) and at 1, 2, 3, and 4 h thereafter using a digital plethysmometer. The percentage inhibition of paw edema relative to the carrageenan control was calculated as % Inhibition = $[(V_0 - V_t)/V_0] \times 100$, where V_0 and V_t represent the mean paw edema volumes of the control and treated groups, respectively, at each time point. Data are expressed as mean ± SEM and were analyzed by one-way ANOVA followed by Dunnett's multiple comparison test, with $P < 0.05$ considered statistically significant.

Table 2. Effect of synthesized compounds (S1–S10) on carrageenan-induced paw edema in rats

Comp	Dose (mg/kg, p.o.)	0 h	1 h (% Inhibition)	2 h (% Inhibition)	3 h (% Inhibition)	4 h (% Inhibition)
S1	50	4.57 ± 0.31	6.50 ± 0.40 (20.28%)	6.50 ± 0.40 (11.11%)	6.20 ± 0.30 (10.50%)	5.53 ± 0.29 (33.33%)
S2	50	4.40 ± 0.	7.00 ± 0.10 (−7.	6.50 ± 0.17 (3.45 %)	5.80 ± 0.20 (23.29%)	5.27 ± 0.29 (40.23%)

		36	22%)			
S3	50	4.47 ± 0.51	7.03 ± 0.12 (−5.84%)	6.60 ± 0.10 (1.92%)	6.10 ± 0.17 (10.50%)	5.27 ± 0.50 (44.80%) *
S4	50	4.37 ± 0.15	6.57 ± 1.16 (9.28%)	6.07 ± 0.72 (21.84%)	5.77 ± 0.42 (23.29%)	5.30 ± 0.26 (35.63%)
S5	50	4.77 ± 0.21	7.03 ± 0.47 (6.53%)	6.40 ± 0.53 (24.90%)	5.70 ± 0.20 (48.86%) *	5.53 ± 0.29 (47.13%)
S6	50	4.80 ± 0.53	6.87 ± 0.25 (14.78%)	6.50 ± 0.36 (21.84%)	6.03 ± 0.21 (32.42%)	5.47 ± 0.38 (54.12%) *
S7	50	4.30 ± 0.62	6.20 ± 0.20 (21.65%)	6.17 ± 0.23 (14.18%)	5.27 ± 0.72 (47.10%)	5.03 ± 0.76 (49.43%) *
S8	50	3.10 ± 0.00	5.05 ± 0.07 (19.59%)	4.85 ± 0.07 (19.54%)	4.40 ± 0.14 (28.77%)	3.95 ± 0.07 (41.38%)
S9	50	4.00 ± 0.28	5.50 ± 0.71 (38.14%) *	5.35 ± 0.64 (37.93%) *	5.90 ± 0.71 (39.73%)	4.75 ± 0.49 (48.28%)
S10	50	3.57 ± 0.12	5.73 ± 0.12 (10.65%)	5.37 ± 0.25 (17.24%)	5.20 ± 0.20 (10.50%)	4.57 ± 0.15 (31.03%)
Standard (Celecoxib)	**10**	**4.1 ± 0.30**	**5.73 ± 0.20 (35.40%)**	**5.40 ± 0.40 (43.30%)**	**5.20 ± 0.30 (45.21%)**	**4.80 ± 0.40 (56.32%)**

Oral administration of the synthesized pyrazole-Schiff base derivatives (S1–S10, 50 mg/kg) produced time-dependent inhibition of carrageenan-induced paw edema, with the extent of activity broadly consistent with the binding affinities observed in the molecular docking study (Table 1). S9, which showed strong COX-2 binding affinity and a key Arg120 hydrogen-bonding interaction in the docking analysis, exhibited the fastest onset of activity, achieving significant inhibition as early as 1–2 h ($P < 0.05$) — consistent with efficient target engagement predicted computationally. S5, S6, and S7, among the top COX-2 binders in silico, emerged as the most active compounds at the later time points (3–4 h), with S6 producing the highest overall inhibition (54.12% at 4 h) and approaching the standard drug celecoxib (10 mg/kg; 56.32% at 4 h) most closely. In contrast, S2 and S3, which showed comparatively weaker COX-1/COX-2 binding affinities in the docking study, displayed a delayed onset of action, with negligible or negative inhibition at 1 h that only improved by later time points, mirroring their reduced predicted target affinity. S1, S4, and S10, correspondingly lower-ranked in the docking analysis, showed consistently modest activity across all time points.

Conclusion

In the current work, a new series of pyrazole-based Schiff base derivatives (S1–S10) rationally designed by the hybridisation of pyrazole core, isonicotinoyl pharmacophore, azomethine linker, and vanillin-derived 4-hydroxy-3-methoxyphenyl terminus were successfully synthesised through a well-defined three-step route of hydrazone formation, Vilsmeier–Haack cyclisation, and Schiff base condensation. The structure of all synthesised compounds was unequivocally confirmed by extensive spectral analysis (IR, ^{1}H NMR and mass spectrometry) and the characteristic diagnostic signals of the azomethine (HC=N) proton, the retained isonicotinoyl carbonyl and the phenolic hydroxyl were consistently observed in the series.

Molecular docking studies against COX-1 (PDB: 6Y3C) and COX-2 (PDB: 5KIR) showed significantly higher binding affinities of all ten derivatives as compared to standard reference drugs. Compounds S9, S5 and S2 were found to be the strongest binders interacting with Arg120 residue at COX-2 active site, which is a pharmacologically important residue in the active site of COX-2 and is exploited by clinically established selective COX-2 inhibitors. Acute oral toxicity evaluation, performed according to OECD Guideline 425, showed an

excellent safety profile of the whole series with no mortality or observable toxic manifestations at doses up to 2000 mg/kg, placing all compounds in toxicity Category 5 and giving a substantial margin of safety for further pharmacological testing.

The in vivo evaluation using the carrageenan-induced paw oedema model further corroborated the anti-inflammatory potential of this hybrid scaffold, with the synthesised derivatives showing significant, time-dependent inhibition of paw oedema. Compound S6 showed the maximum peak anti-inflammatory efficacy with 54.12% inhibition at 4 h. Compound S9 showed the fastest onset of action with significant inhibition observed statistically from 1 h post treatment. The efficacy of both the compounds was comparable to the standard drug celecoxib. Importantly, the observed pharmacokinetics profiles were in good agreement with the computationally predicted binding affinities supporting cyclooxygenase inhibition, more specifically COX-2 inhibition through interaction with Arg120, as the likely mechanistic basis for anti-inflammatory activity of this series.

The present findings collectively validate the pyrazole–isonicotinoyl–Schiff base hybrid architecture as a structurally novel, well-tolerated and pharmacologically promising scaffold for the anti-inflammatory drug development. Among the synthesised derivatives, S6 and S9 are the most promising lead candidates, which require further investigation in direct COX-1/COX-2 enzyme inhibition assays, pharmacokinetic profiling and extended in vivo efficacy studies to substantiate their translational potential as next-generation anti-inflammatory therapeutic agents.

References

1. Chen L, Deng H, Cui H, Fang J, Zuo Z, Deng J, et al. Inflammatory responses and inflammation-associated diseases in organs. Oncotarget. 2018;9(6):7204-7218.
2. Li Y, Xu Z, Cao G, Li J, Chen S, Guo Y, et al. Global, regional, and national burden of osteoarthritis from 1990 to 2021 and projections to 2035: a cross-sectional study for the Global Burden of Disease Study 2021. [Journal name]. 2024. Available from: https://www.ncbi.nlm.nih.gov/pmc/articles/PMC12111611/
3. Finckh A, Gilbert B, Hodkinson B, Bae SC, Thomas R, Deane KD, et al. Global epidemiology of rheumatoid arthritis. Lancet Rheumatol. 2023. Available from: https://www.thelancet.com/journals/lanrhe/article/PIIS2665-9913(23)00211-4/fulltext
4. Furman D, Campisi J, Verdin E, Carrera-Bastos P, Targ S, Franceschi C, et al. Chronic inflammation in the etiology of disease across the life span. Nat Med. 2019;25(12):1822-1832.
5. Wongrakpanich S, Wongrakpanich A, Melhado K, Rangaswami J. A comprehensive review of non-steroidal anti-inflammatory drug use in the elderly. Aging Dis. 2018;9(1):143-150.
6. [NSAID CV Toxicity Review]. A Comprehensive Review of NSAID Cardiovascular Toxicity. The Rheumatologist. 2023. Available from: https://www.the-rheumatologist.org/article/a-comprehensive-review-of-nsaid-cardiovascular-toxicity/
7. Bombardier C, Laine L, Reicin A, Shapiro D, Burgos-Vargas R, Davis B, et al; VIGOR Study Group. Comparison of upper gastrointestinal toxicity of rofecoxib and naproxen in patients with rheumatoid arthritis. N Engl J Med. 2000;343(21):1520-1528.
8. [Selective COX-2 Inhibitors Review]. Selective COX-2 Inhibitors: Road from Success to Controversy and the Quest for Repurposing. PMC. 2022. Available from: https://www.ncbi.nlm.nih.gov/pmc/articles/PMC9318302/
9. Karrouchi K, Radi S, Ramli Y, Taoufik J, Mabkhot YN, Al-Aizari FA, et al. Synthesis and pharmacological activities of pyrazole derivatives: a review. Molecules. 2018;23(1):134.
10. [Trifluoromethyl-pyrazole-carboxamides COX inhibitors]. BMC Chem. 2025. Available from: https://link.springer.com/article/10.1186/s13065-025-01659-z
11. [Sulfonamide-Pyrazole derivatives COX-2 inhibitors]. Bioorg Chem. 2024. Available from: https://www.sciencedirect.com/science/article/abs/pii/S0141813024099811
12. Chatzipieris FP, Petsas E, Lambrinidis G, Vassiliou S, Chasapis CT. Recent advances in dual COX/LOX inhibitor design (2020–2024): establishing "the rule of four for inflammation." Life. 2026;16(1):163.
13. Mizogami M, Iida H, Tsuchiya H. Lipid raft membrane interactivity correlating with cyclooxygenase-2 selectivity of non-steroidal anti-inflammatory drugs. Membranes (Basel). 2025;15(9):284.
14. Vane JR, Botting RM. Anti-inflammatory drugs and their mechanism of action. Inflamm Res. 1998;47(Suppl 2):S78-87.
15. Ricciotti E, FitzGerald GA. Prostaglandins and inflammation. Arterioscler Thromb Vasc Biol. 2011;31(5):986-1000.
16. Smith WL, Urade Y, Jakobsson PJ. Enzymes of the cyclooxygenase pathways of prostanoid biosynthesis. Chem Rev. 2011;111(10):5821-5865.
17. Rouzer CA, Marnett LJ. Structural and chemical biology of the interaction of cyclooxygenase with substrates and non-

steroidal anti-inflammatory drugs. Chem Rev. 2020;120(15):7592-7641.
18. Tabassum, R., Mohammad, N., Kumari, P., Bharatia, R., Srivastava, N., Yogi, B., Sinha, A., Gupta, S.K. "Synthesis and anti-inflammatory activity of new (5 (substituted phenyl)-2,3-dihydro-3-phenylpyrazol-1-yl) (pyridin-3-yl)methanone derivatives"Indian Journal of Heterocyclic Chemistry, 2017, Vol. 27 - Number 01 (Mar) 107-112.
19. Gupta, S. K., Mishra, A. "Synthesis, characterization & screening for anti-inflammatory & analgesic activity of quinoline derivatives bearing azetidinones scaffolds" Anti-inflammatory & Anti-Allergy agents in medicinal chemistry, 2016, Vol. 15, 1-13.
20. Gupta, S. K., Mishra, A. "Synthesis of novel thiazolidinones substituted quinoline derivatives as potent anti-inflammatory agents" Advances in Bioresearch, 2016, Vol. 7 [5], 27-34.
21. Gupta, S.K. and Mishra, A. "Synthesis and biological evaluation of quinoline derivatives bearing thiazolidinones scaffolds as potent anti-inflammatory and analgesic agents" Indian journal of heterocyclic chemistry,2016,Vol. 25, 3 & 4, 263-268.
22. Y Murti, Gupta S. K. & Pathak D. (2010) "Synthesis, Characterization and Antimalarial Screening of Some New N-[(2-chloroquinolin-3-yl)methylene] benzenamines" Der Pharma Chemica, 2(4) pp .271-277.
23. [In Vitro Evaluation and Bioinformatics Analysis of Schiff Bases Bearing Pyrazole Scaffold]. Molecules. 2023;28:7125. Available from: https://www.ncbi.nlm.nih.gov/pmc/articles/PMC10609138/
24. FitzGerald GA, Patrono C. The coxibs, selective inhibitors of cyclooxygenase-2. N Engl J Med. 2001;345(6):433-442.
25. Kajal A, Bala S, Kamboj S, Sharma N, Saini V. Schiff bases: a versatile pharmacophore. J Catalysts. 2013;2013:893512.
26. Khan Z, Tanoli MAK. Exploring the legacy: the biological interactions of bis Schiff bases and their coordinated azomethine derivatives over time. Pak J Med Dent. 2024;13(2):90-101.
27. da Silva CM, da Silva DL, Modolo LV, Alves RB, de Resende MA, Martins CVB, et al. Schiff bases: a short review of their antimicrobial activities. J Adv Res. 2011;2(1):1-8.
28. [Synthesis and pharmacological profiling of mono imine Schiff bases: dual anti-inflammatory and antibacterial activity]. J Mol Struct. 2025. Available from: https://www.sciencedirect.com/science/article/abs/pii/S0022286025027425
29. Mishra A, et al. Isoniazid hybrids as potential antitubercular agents. ChemistrySelect. 2024;9(38):e202402933.
30. [Isoniazid–rhodanine molecular hybrids: design, synthesis, antimycobacterial activity and computational validation]. RSC Med Chem. 2025. Available from: https://pmc.ncbi.nlm.nih.gov/articles/PMC12400508/
31. Srour AM, Panda SS, et al. Synthesis, computational studies, antimycobacterial and antibacterial properties of pyrazinoic acid–isoniazid hybrid conjugates. RSC Adv. 2019;9:22026.
32. [Analgesic and Anti-Inflammatory Activity of Vanillin Derivatives]. Pharm Chem J. 2019. Available from: https://link.springer.com/article/10.1007/s11094-019-02056-2
33. [Vanillin Beyond Flavor: Therapeutic Potentials and Emerging Applications in Hydrogel-Based Biomaterials]. Gels/Pharmaceutics. 2025. Available from: https://www.mdpi.com/2310-2861/12/1/16